DOI: 10.19884/j.1672-5220.202507002

A Combination-Driven Radiation Source Seeking Algorithm Based on Improved SPSA

LI Guanru[1], HU Jun[2,3*], YU Zhou[2], ZHU Shijie[4]
1. College of Mechanical Engineering, Donghua University, Shanghai 201620, China
2. Institute of Artificial Intelligence, Donghua University, Shanghai 201620, China
3. Engineering Research Center of Artificial Intelligence for Textile Industry, Ministry of Education, Institute of Artificial Intelligence, Donghua University, Shanghai 201620, China
4. School of Information and Intelligent Science, Donghua University, Shanghai 201620, China

Abstract: In response to the challenges of radiation source localization in shielded environments, a combination-driven algorithm is proposed based on an improved simultaneous perturbation stochastic approximation (SPSA) framework. The proposed algorithm enhances the convergence performance by optimizing one-sided orthogonal perturbation vectors and incorporating a dynamic step-size adjustment strategy. To address path infeasibility in complex environments, a goal relocation mechanism based on breadth-first search (BFS) is introduced. For complex multi-space scenarios with shielding structures, an active exploration strategy is employed to proactively investigate unobserved regions. To evaluate the performance of the proposed algorithm in terms of convergence performance, obstacle adaptability, and exploration capacity, three simulation environments are set up in Gazebo, which respectively represent the following environments: open-field environment, complex environment and radiation shielding environment. The experiments demonstrate that the proposed algorithm outperforms the standard SPSA algorithm and particle filter algorithm in terms of convergence performance, while also exhibiting robust search capability in complex environments. Furthermore, when confronted with shielded environments, the proposed algorithm demonstrates the capability of actively exploring unknown areas within a relatively short period after being obstructed.

Keywords: source seeking algorithm; simultaneous perturbation stochastic approximation; combination-driven algorithm; active exploration
CLC number: TL81 **Document code**: A
Article ID: 1672-5220(2026)04-0110-09

0 Introduction

Nuclear technology has developed for over a century since its discovery and is extensively utilized across multiple domains including national defense construction, industrial testing, medical diagnostics and treatment, and environmental monitoring. It continues to play an irreplaceable role in societal development and technological advancement[1-2].

With the increasing utilization of radioactive materials, accidents associated with them are also occurring. Such as the Chernobyl accident[3] and the Fukushima Daiichi nuclear power plant accident[4]. Therefore, the technology of locating and searching for uncontrolled radioactive sources has become a key technology in dealing with nuclear radiation incidents.

In recent years, the rapid development of robotics has drawn increasing attention to machine-assisted radioactive source search[5], which has shown strong application potential in areas such as post-disaster rescue and nuclear safety[6]. In the field of source localization, related source seeking algorithms are typically classified into three categories based on their decision-making strategies: control-driven, information-driven, and combination-driven algorithms[7].

Extremum-seeking algorithms are the predominant algorithms among control-driven algorithms. Their typical structure employs perturbation signals to estimate the gradient of the objective function and update the tuning parameters, guiding the objective function toward its extremum. Xu et al.[8] demonstrated that for the source search system, normalized extremum seeking had better robustness than general extremum seeking by building a single-round odor search system. Ramírez et al.[9] proposed a control-driven algorithm based on stochastic gradient estimation by using the simultaneous perturbation stochastic approximation (SPSA) algorithm to guide the mobile robot toward the signal source and theoretically demonstrated that the SPSA algorithm is effective in source seeking applications. Chen et al.[10] proposed a normalized extremum-seeking control method for unmanned aerial vehicle (UAV) swarm-based source seeking, in which the source localization task was reformulated as an extremum-seeking problem over an unknown artificial potential field. However, despite these

Received date: 2025-07-14
* Correspondence should be addressed to HU Jun, email: hjmorning@hotmail.com
Citation: Li G R, Hu J, Yu Z, et al. A combination-driven radiation source seeking algorithm based on improved SPSA [J]. *Journal of Donghua University (English Edition)*, 2026, 43(4): 110-118.

advances, control-driven algorithms still face challenges, as they often become trapped in local optima on one side of the obstacle due to limited environmental sensitivity[11]. Therefore, enhancing the adaptability of such algorithms across diverse environments remains a valuable research challenge.

The current mainstream information-driven algorithms primarily rely on a Bayesian estimation framework to estimate parameters associated with radiation sources. Zhang et al.[12] combined the artificial field potential method with particle filtering to propose a source finding algorithm with higher search efficiency and verified that the algorithm still had effective results in open environments. Hutchinson et al.[13] combined a Bayesian inference engine with the information theory for path planning and demonstrated its effectiveness in real-world experiments. However, in real-world environments, estimation algorithms such as particle filtering face challenges in accurate modeling due to environmental shielding effects on radioactive sources, making them susceptible to interference from shielding and resulting in biased parameter estimates[14]. Meanwhile, algorithms that emphasize environmental exploration to gather information for source localization have also attracted considerable attention. Long et al.[15] estimated the source's actual location by discretizing a continuous radiation field and inversely solving for the source intensity with data collected from detection points. However, the most explorable regions are often not the actual source regions, resulting in such algorithms achieving better environmental estimation but not necessarily yielding accurate source localization results[16].

Combination-driven algorithms establish a unified framework that balances exploration and exploitation by integrating control-driven feedback mechanisms with information-driven source parameter estimation. Li et al.[17] have proposed a dual control algorithm for exploration and exploitation (DCEE) for locating airborne pollution sources in unknown environments. This algorithm employs extreme value search and parameter estimation to promote each other without interference. Although DCEE achieves a favorable balance between efficiency and accuracy, in the context of radioactive source search, the parameter estimation component may not always contribute effectively and can, in some cases, reduce overall search efficiency.

In summary, due to the penetrative nature of radioactive sources, the task of radioactive source search presents more complex challenges than odor tracking. Moreover, algorithms capable of maintaining robust performance in environments with shielding objects remain limited. To address these issues, this paper proposes a combination-driven algorithm based on an improved SPSA. The proposed algorithm integrates both sensing and exploration mechanisms, in order to address the slow convergence and poor robustness exhibited by conventional SPSA in varying radiation field conditions, and significantly enhances the accuracy of source localization in shielded environments.

1 Algorithm Design

SPSA is a stochastic gradient estimation algorithm by perturbing all parameters simultaneously. The robot is parameterized in two dimensions by its position $\boldsymbol{p} = (x, y)$, where x and y denote the coordinates on a plane, and $\boldsymbol{p} \in \mathbf{R}^2$ indicates that the position vector lies in the two-dimensional real coordinate space. The radiation sensor signal strength at that position at the kth iteration $s_k = f(\boldsymbol{p}_k) = f(x_k, y_k)$, where $f(\cdot)$ is unknown radiation field dose distribution. The current position strength can be measured by the sensor.

A random perturbation vector at the kth iteration following a Bernoulli distribution is introduced:

$$\boldsymbol{\Delta}_k = \begin{bmatrix} \Delta_{k1} \\ \Delta_{k2} \end{bmatrix}, \ \Delta_{k1}, \Delta_{k2} \in \{-1, 1\}, \tag{1}$$

where Δ_{k1} and Δ_{k2} are stochastic perturbation variables along two dimensions at the kth iteration.

Assuming that the robot is at position $\boldsymbol{p}_k$, the estimated gradient of the radiation field $\hat{\nabla} f(\boldsymbol{p}_k)$:

$$\hat{\nabla} f(\boldsymbol{p}_k) = \frac{f(\boldsymbol{p}_k + \delta \cdot \boldsymbol{\Delta}_k) - f(\boldsymbol{p}_k - \delta \cdot \boldsymbol{\Delta}_k)}{2\delta} \cdot \boldsymbol{M}_k, \tag{2}$$

where δ is the perturbation step; $\boldsymbol{M}_k$ is a reconstruction vector associated with the sampling direction, and used to map the scalar variations measured by sensors into a gradient estimation vector within the x-y coordinate.

Subsequently, the current position parameter $\boldsymbol{p}_{k+1}$ is updated based on this gradient estimate:

$$\boldsymbol{p}_{k+1} = \boldsymbol{p}_k + s_k \hat{\nabla} f(\boldsymbol{p}_k), \tag{3}$$

where s_k is the step size at the kth iteration, typically defined as a decreasing sequence satisfying the Robbins-Monro conditions in the SPSA algorithm. $s_k = \frac{a}{(k + 1 + A)^{\alpha}}$, where a is the initial learning rate, which scales the overall step size; A is the stability constant, often set to a small fraction of the total iterations, to prevent excessively large steps in the initial iterations; α is the decay exponent, controlling the asymptotic decay rate of the step size. a, k, A and α are adjustable hyperparameters.

The traditional SPSA algorithm, in linear function scenarios, typically converges rapidly to the global optimum within a fixed number of iterations by applying bilateral perturbations to the parameters for gradient estimation. However, real radiation environments are non-ideal. In a standard radiation field, the intensity generally follows the inverse square law, and according to the point kernel method[18], the intensity $S(\boldsymbol{p}_k \mid \psi_s)$ of a point source ψ_s at a given location can be expressed as

$$S(\boldsymbol{p}_k \mid \psi_s) = \frac{\psi_{s,\,str}}{(\boldsymbol{p}_k - \boldsymbol{\psi}_{s,\,pos})^2} \cdot B \cdot e^{-\mu d}, \qquad (4)$$

where μ is the linear attenuation coefficient of the obstacle (m^{-1}); d is the thickness of the obstacle (m); $\boldsymbol{\psi}_{s,\,pos}$ is the location of the point source; $\boldsymbol{\psi}_s$ is the radiation intensity measured by a Geiger Müller counter at 1 m from the point source (μSv/h); B is the build-up factor due to scattering by the obstacleoint source.

The traditional SPSA algorithm exhibits notable limitations in radiation field environments. Specifically, its performance is highly sensitive to hyperparameters, limiting its adaptability and making it challenging to achieve both rapid convergence and precise localization in source seeking tasks. Furthermore, as a control-driven algorithm, it relies solely on current sensor data and lacks active exploration capability, making it prone to local optima in shielded environments, thereby significantly reducing both the efficiency and success rate of radioactive source localization.

To address the aforementioned limitations, the improved SPSA algorithm proposed in this paper incorporates three key components. First, based on the SPSA algorithm, improved strategies for generating perturbations and step control are proposed and employed. Second, to address the issue of goal points or sampling points falling into impassable regions in unknown environments, a target point correction mechanism based on breadth-first search (BFS) is introduced. Finally, an active exploration mechanism tailored to shielded environments is proposed to enhance the algorithm's exploration capability. A flowchart of the improved SPSA algorithm is presented in Fig. 1.

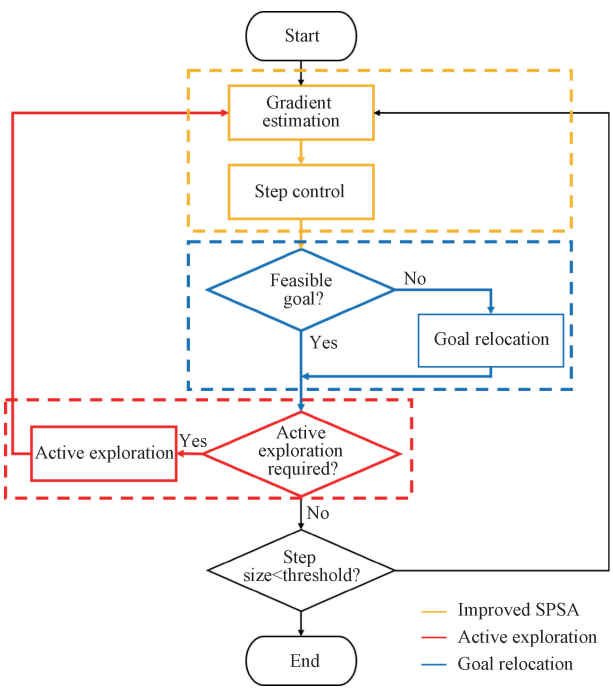


Fig. 1 Flowchart of improved SPSA algorithm

1.1 Improved SPSA algorithm

1.1.1 Enhanced gradient estimation

The SPSA algorithm typically employs a perturbation vector following a Bernoulli distribution, with elements being restricted to ±1. As a result, the perturbation directions are confined to the orthogonal axes of the coordinate system. The limited directional diversity in the perturbation vector adversely affects the algorithm's performance in complex optimization spaces.

At the kth iteration, to estimate the gradient of an n-dimensional scalar field, the improved SPSA algorithm introduces a set of m orthogonal perturbation vectors $\boldsymbol{\Delta}$ with n components:

$$\{\boldsymbol{\Delta}_{1,k}, \boldsymbol{\Delta}_{2,k}, \cdots, \boldsymbol{\Delta}_{m,k}\} \in \mathbf{R}^{n\times m},\ m \leqslant n. \qquad (5)$$

Instead of employing traditional independent random perturbation vectors, the perturbation directions are designed to be more uniformly informative across each dimension, thereby reducing the variance of gradient estimation and enhancing algorithm stability. In this paper, we further impose a unit norm constraint by normalizing the perturbation vectors onto the unit hypersphere. For each vector $\boldsymbol{\Delta}_{i,k}$ in the set,

$$\|\boldsymbol{\Delta}_{i,k}\|_2 = 1,\ i \leqslant m. \qquad (6)$$

In view of the high response speed and resource constraints inherent to the radiation source search task, the gradient estimation is improved by employing a one-sided orthogonal SPSA algorithm that reduces sampling overhead during the gradient estimation process:

$$\hat{\nabla} f(\boldsymbol{p}_k) = \frac{1}{m}\sum_{i=1}^{m} \frac{f(\boldsymbol{p}_k + \delta \cdot \boldsymbol{\Delta}_{i,k}) - f(\boldsymbol{p}_k)}{\delta} \cdot \boldsymbol{M}_k. \qquad (7)$$

The aforementioned modifications enhance the algorithm's stability without increasing the sample size, while also broadening the selection space of random perturbations.

1.1.2 Dynamic step control

To balance the requirements of rapid local convergence and global approximation in the radiation source localization task, this paper proposes a dynamic step control mechanism. The mechanism dynamically updates the robot's advancement step size based on gradient-based information and optimal value guidance.

If the step size at iteration t is s_t, the current estimated gradient of the improved SPSA algorithm is $\boldsymbol{g}_t = [g_{x,t} \quad g_{y,t}]$, the historically optimal sensor measurement position is $\boldsymbol{p}_{opt}$, and the previous iteration's gradient is $\boldsymbol{g}_{t-1} = [g_{x,t-1} \quad g_{y,t-1}]$. The directional consistency between the two gradients is evaluated via their dot product. When the dot product is negative, namely, $\boldsymbol{g}_t \cdot \boldsymbol{g}_{t-1} < 0$, it indicates a significant deflection between the current and previous estimated gradient directions, suggesting that the robot may have crossed the radioactive source location or encountered a local extremum. In such cases, the step

size should be appropriately reduced:

$$s_t = s_{t-1} \cdot \rho,\ 0 < \rho < 1, \tag{8}$$

where ρ is the reversal attenuation coefficient.

If $\boldsymbol{g}_t$ is directionally consistent with $\boldsymbol{g}_{\text{opt}}$:

$$\arccos\left(\frac{\boldsymbol{g}_t \cdot \boldsymbol{g}_{\text{opt}}}{\|\boldsymbol{g}_t\| \cdot \|\boldsymbol{g}_{\text{opt}}\|}\right) < \frac{\pi}{6}, \tag{9}$$

where $\boldsymbol{g}_{\text{opt}}$ is the vector from the current position to $\boldsymbol{p}_{\text{opt}}$.

Then the current direction is basically consistent with the historically optimal response direction, and the step size can be further contracted for fine search:

$$s_t = s_{t-1} \cdot \rho \cdot \sigma,\ 0 < \rho < 1,\ 0 < \sigma < 1, \tag{10}$$

where σ is the fine search correction factor.

If no gradient reversal is detected, the step size gradually increases to accelerate convergence:

$$s_t = s_{t-1} \cdot \gamma,\ \gamma > 1, \tag{11}$$

where γ is the step size growth factor.

When the step size falls below the threshold s_{thre}, the algorithm terminates and returns the historical optimal location as the estimated source location.

1.2 Goal relocation mechanism

During the source localization process, the goal and sampling location computed by the improved SPSA algorithm may not always lie within the reachable space, particularly in complex environments. To address this issue, this paper introduces a goal relocation mechanism based on BFS, which dynamically adjusts the goal point position under obstacle constraints.

During the homing task, the mobile robot perceives its surroundings by maintaining a grid map Ω. When the goal point $\boldsymbol{p}_{\text{goal}}$ generated by the gradient estimation module is determined to lie within an impassable region Ω_{obs}:

$$\boldsymbol{p}_{\text{goal}} \in \Omega_{\text{obs}}. \tag{12}$$

The algorithm initiates a BFS search on Ω centered at this point. It adds the $\boldsymbol{p}_{\text{goal}}$ to the search queue l_{BFS} and performs the following operations on each element within the queue:

1) If $l_{\text{BFS}} \cap \Omega_{\text{free}} = \varnothing$, its Moore neighborhood positions on the map are examined. Valid neighboring positions are added to the queue, and the search continues.

2) If such coordinates $\boldsymbol{p}_{\text{goal, f}}$ are found, $\boldsymbol{p}_{\text{goal, f}} \in \Omega_{\text{free}}$, s. t. $\|\boldsymbol{p}_{\text{goal, f}} - \boldsymbol{p}_{\text{r}}\| < d_{\text{thre}}$, the search is terminated, and the corresponding point is used to replace the original goal point as the new navigation goal. Here d_{thre} is the distance threshold and Ω_{free} is the accessible region.

The goal relocation mechanism is shown in Fig. 2.

The robot successfully reaches a feasible nearby location by invoking a goal correction mechanism when its original target is identified as an obstacle.

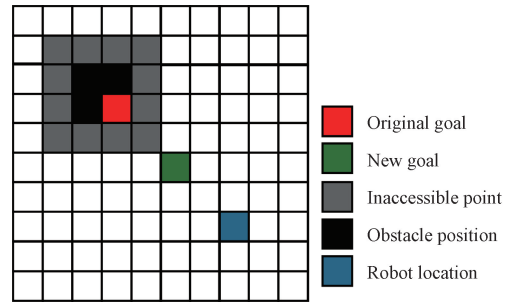


Fig. 2 Illustration of goal relocation

1.3 Active exploration strategy

In the real world, the robot and the radioactive source may not always be located within the same unobstructed space, as shielding materials can significantly attenuate sensor readings.

The radiation field effect of a highly shielded T-shaped concrete wall with a thickness of 0.2 m, a linear attenuation coefficient of 21.5 m^{-1}, and a buildup factor B of 12.5 on a radioactive source with a dose rate of 8 000 μSv/h is shown in Fig. 3.

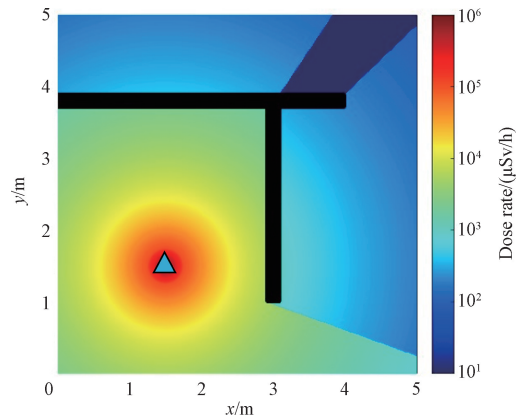


Fig. 3 Radiation field distribution under shielding conditions

To enhance the algorithm's exploration capacity in shielded environments and address the limitations of the SPSA algorithm, this paper proposes an active exploration strategy.

Let the current estimated target location be denoted by $\boldsymbol{p}_{\text{goal}}$, and the robot location by $\boldsymbol{p}_{\text{r}}$. When the active exploration is triggered, the active exploration strategy constructs a candidate set F of frontier points. These points are defined as the intersection of the accessible region and the unknown region Ω_{unk}, within a neighborhood of a radius r centered at $\boldsymbol{p}_{\text{goal}}$:

$$F = \{x_i \in \Omega_{\text{unk}} \mid B(x_i) \cap \Omega_{\text{free}} \neq \varnothing\}, \tag{13}$$

where $B(x_i)$ is the Moore neighborhood centered at x_i.

A clustering operation is performed on the candidate frontier point set to merge adjacent frontier points into frontier regions F. The resulting set of frontier regions is denoted as G. For any two candidate regions G_i and G_j, they are non-overlapping.

$$G = \{G_1, \cdots, G_i, \ldots G_j, \cdots, G_n\}, \bigcup_{i=1}^{n} G_i = F,$$
$$G_i \cap G_j = \varnothing, \ i \neq j. \tag{14}$$

For each frontier region midpoint $\boldsymbol{x}_{i,\mathrm{m}} \in G_{\mathrm{m}}$, G_{m} is the set of region midpoints corresponding to the set of frontier regions G and compute its cost:

$$C(\boldsymbol{x}_{i,\mathrm{m}}) = \sigma \cdot c_{\mathrm{d}}(\boldsymbol{x}_{i,\mathrm{m}}, \boldsymbol{p}_{\mathrm{goal}}) + \beta \cdot c_{\mathrm{s}}(\boldsymbol{x}_{i,\mathrm{m}}), \tag{15}$$

where $c_{\mathrm{d}}(\boldsymbol{x}_{i,\mathrm{m}}, \boldsymbol{p}_{\mathrm{goal}})$ denotes the cost function representing the distance from a point within the region to the target point; $c_{\mathrm{s}}(\boldsymbol{x}_{i,\mathrm{m}})$ denotes the cost function representing the size of the region; σ and β are the weighting parameters.

The frontier point with the lowest total cost is then selected from the candidate set as the exploration location:

$$p_{\mathrm{expl}} = \arg\min_{\boldsymbol{x}_{i,\mathrm{m}} \in G_{\mathrm{m}}} C(\boldsymbol{x}_{i,\mathrm{m}}). \tag{16}$$

A schematic of the active exploration strategy is shown in Fig. 4.

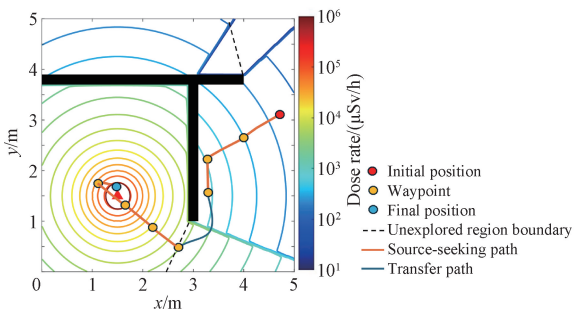


Fig. 4 Schematic of active exploration strategy

After taking two steps from the initial position, the robot is obstructed by the shield, which activates the exploration mechanism and drives it toward the boundary of the perceptual map (indicated by the dotted line). Upon completing this transition, the robot reinitializes the algorithm and successfully localizes the radioactive source.

2 Simulation Experiments

To comprehensively evaluate the performance of the algorithm proposed in this paper under various radioactive source search environments, three experimental environments are designed based on the Gazebo simulation platform. The simulated radioactive source follows Eq. (4) with a source dose rate of 40 000 μSv/h. The improved algorithm is evaluated in terms of convergence performance, obstacle adaptability, and exploration capacity through the following settings:

1) Ideal open-field environment. The robot starts from a distance, and a comparative experiment is conducted among the traditional SPSA algorithm, the improved SPSA algorithm, and the particle filter algorithm.

2) Outdoor complex environment. Multiple obstacles are randomly distributed. Although these obstacles exert negligible attenuation on the radiation emitted by the source, they increase the complexity of the robot's search process and are used to evaluate the algorithm's obstacle-handling capability.

3) Radiation shielding environment. A scenario simulating real indoor environments with shielding objects is constructed to evaluate the exploration capability of the algorithm.

Each experiment was repeated 20 times to collect statistical results.

To optimize the performance of the proposed algorithm across varied operational environments, the following key parameters were carefully configured. An initial step size of 3.0 m coupled with a step size growth factor of 1.05 is employed. For convergence refinement, a reversal attenuation coefficient of 0.75 is integrated with a fine search correction factor of 0.66. This synergistic combination promotes fast and stable convergence near the true source location, avoiding the misjudgments and efficiency degradation associated with an inappropriately large reversal attenuation factor. The termination threshold and sampling step size were empirically determined to balance task accuracy requirements with the practical performance constraints of the robotic platform. This parameterization ensures a final positioning accuracy higher than 0.5 m and maintains better robustness against inherent robot localization and navigation errors. The parameter settings of the proposed algorithm are listed in Table 1.

Table 1 Parameters of improved SPSA algorithm

Simulation parameter	Value
Initial step size s_0/m	3.0
Sampling step size δ/m	0.5
Reversal attenuation coefficient ρ	0.75
Fine search correction factor σ	0.66
Step size growth factor γ	1.05
Step size termination threshold s_{thre}/m	0.8

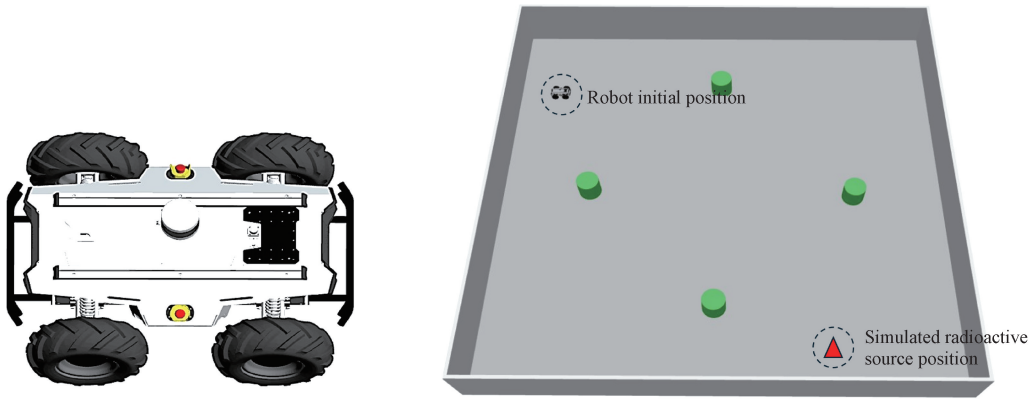
2.1 Experiment in open-field environment

To evaluate the convergence performance of the proposed algorithm in the open-field environment, a simulation environment of 20 m × 20 m was established using the Gazebo platform. The robot model in the simulation and the simulation open-field environment are shown in Fig. 5.

To ensure the consistency, the initial step size of the SPSA algorithm used for comparison was set to match that of the proposed algorithm. Specifically, a is 6, A is 3, and α is 0.602. The algorithm terminates when the step size falls below 1.0 m.

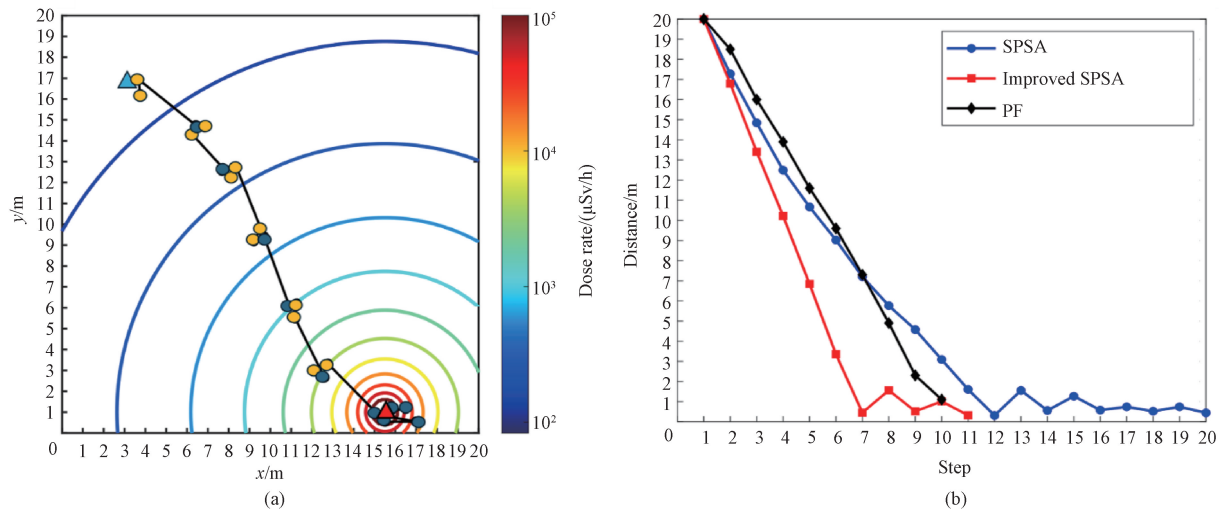
For the particle filter (PF) based source search algorithm, a comparative experiment was also conducted under the same environmental and initial conditions. The PF algorithm was implemented with 500 particles and terminated when the current position and the estimated source position of the robot both fell below 0.8 m. The

simulation results in the open-field environment are shown in Fig. 6



(a) (b)

Fig. 5 Simulation model and environment in Gazebo for experiment in open-field environment: (a) robot model; (b) simulation open-field environment



(a) (b)

Fig. 6 Results in open-field environment: (a) improved SPSA algorithm path illustration; (b) step-distance comparison among SPSA, improved SPSA and PF algorithms

Table 2 summarizes various metrics recorded during the experimental process, including the average error of the algorithm, the convergence step (the number of iterations required for the robot to the first reach within 1.0 m of the radioactive source), and the average steps (the total number of steps taken to complete the source seeking task).

Table 2 Results of simulation experiment in open-field environment

Algorithm	Average error/m	Average convergence step	Average step
SPSA	1.23	11.45	20.0
Improved SPSA	0.28	6.25	10.3
PF	1.06	8.90	9.3

Owing to the fundamental differences in their implementation principles, the average steps at termination cannot serve as a direct metric for comparing the efficiency of PF and improved SPSA algorithms. Therefore, this study focuses on the core metric of the approach efficiency under the same movement steps.

Driven by the combined effect of enhanced gradient estimation and a dynamic step control strategy, the improved SPSA algorithm demonstrates a significantly superior approach speed in the open-field environment compared to the other two methods: the SPSA algorithm requires an average of 11.45 steps to reach within 1.0 m of the radiation source, while the improved SPSA algorithm achieves the same proximity within only 7 steps, and the PF algorithm requires about 9 steps to approach the target vicinity. These results indicate that the improved SPSA algorithm achieves an effective balance between the rapid approach and accurate convergence, thereby enhancing both the efficiency and robustness.

2.2 Experiment in outdoor complex environment

To further test the obstacle adaptability of the proposed algorithm in the outdoor complex environment, this paper randomly distributes some obstacles on the basis of the experiment in the open-field environment, as shown in Fig. 7.

The radioactive source was placed at the same location as in the simulation experiment in the open-field environment, while the mobile robot was randomly positioned 20 m away in the upper-left corner. Table 3 summarizes the average number of steps, average error, relocation success rate of the BFS mechanism, and the number of relocations. Figure 8 shows sample execution paths of the mobile robot during two experiments.

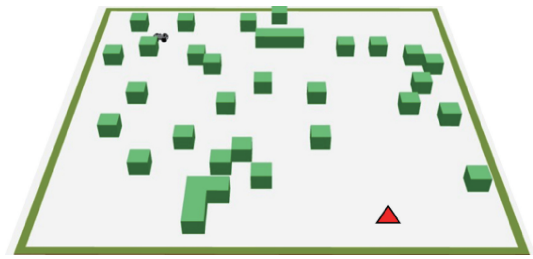


Fig. 7 Simulation environment with complex obstacles

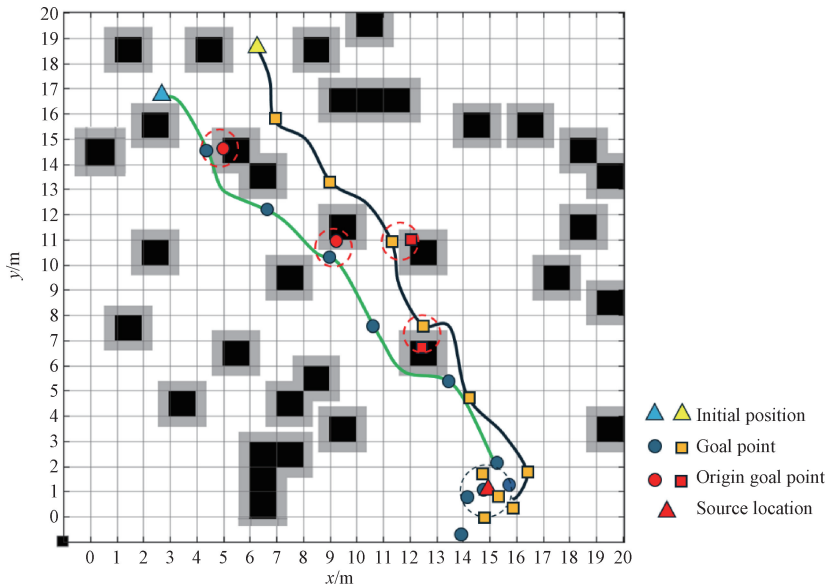


Fig. 8 Path illustration for simulation experiment in outdoor complex environment

Table 3 Results of simulation experiment in outdoor complex environment

Parameter	Average step	Average error/m	Relocation success rate	Average number of relocations
Value	12.2	0.33	0.39	4.35

As shown in Fig. 8, although the improved SPSA algorithm places the target point in inaccessible regions at the red-circled location s, the proposed goal relocation mechanism successfully relocates the target locations to the neighboring accessible locations. This mechanism ensures the feasibility of the source seeking path without substantially altering the search direction. Table 3 indicates that, compared to the experiment in the open-field environment, the average steps increase by 1.9, demonstrating that the improved SPSA algorithm maintains high accuracy and stability even in an outdoor complex environment with obstacles.

2.3 Experiment in radiation shielding environment

To evaluate the exploration capacity of the improved SPSA algorithm in radiation shielding environments, an indoor site (15 m × 15 m) was simulated with walls (0.2 m in thickness), a linear attenuation coefficient of 14.3 m^{-1}, and a shielding cumulative factor B of 10.5. The radioactive source was placed in the lower-left room, while the robot started from the upper-left room. The simulation setup and radiation dose rate distribution are shown in Fig. 9.

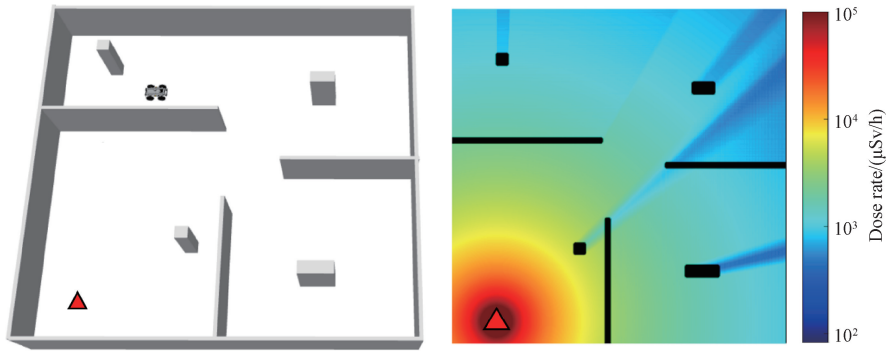


Fig. 9 Simulation environment with shielding structures: (a) simulation radiation shielding environment in Gazebo; (b) radiation dose rate distribution

Figure 10 shows the path of the mobile robot in the inflated map in one of the simulation experiments.

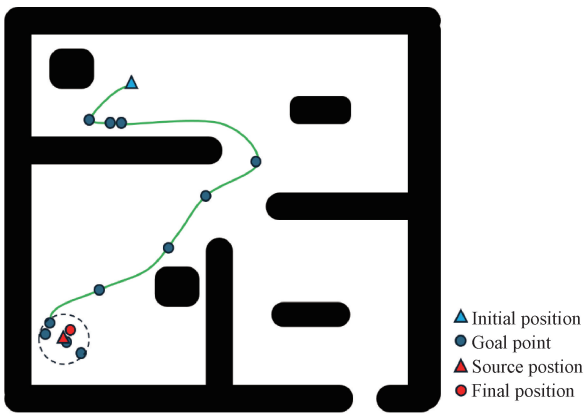


Fig. 10 Path illustration for simulation experiment in radiation shielding environment

Table 4 presents data for four evaluation metrics. When the robot is obstructed by shielding objects and remains at a non-source location, the active exploration strategy enables it to actively explore the frontier region closest to the source. This allows the robot to subsequently successfully find the radioactive source location. The robot requires less than three steps on average to trigger exploration and successfully migrate to the opposite side, demonstrating the effectiveness of the improved SPSA algorithm in the radiation shielding environment.

Table 4 Results of simulation experiment in radiation shielding environment

Parameter	Average error/m	Average step	Exploration trigger step	Step distribution probability for exploration trigger/%	
				≤3 step	>3 step
Value	0.31	12.6	2.2	85	15

3 Conclusions

In this study, we propose an improved SPSA algorithm that integrates sensing and exploration to address the limited robustness of existing source seeking methods in radiation shielding environments. Compared to the traditional SPSA algorithm, the proposed algorithm significantly enhances the convergence performance in standard radiation fields. To handle environments with obstacles, a goal relocation mechanism is introduced to improve the feasibility of the planned path. In radiation shielding environments, the active exploration strategy compensates for localization errors caused by sensing limitations, thereby improving the algorithm's adaptability and robustness. However, in high-density shielding conditions, the accuracy of gradient estimation degrades significantly due to the reduced penetrability of radioactive sources, indicating that further improvement is needed. Overcoming the limitations of penetration to enable robust gradient sensing remains a critical challenge for future research.

References

[1] Xiao W. Current status and safeguard measures of nuclear industry development [J]. *Papermaking Equipment & Materials*, 2020, 49(2): 252. (in Chinese)

[2] Miernicki E A, Heald A L, Huff K D, et al. Nuclear waste heat use in agriculture: history and opportunities in the United States [J]. *Journal of Cleaner Production*, 2020, 267: 121918.

[3] Hatch M, Ron E, Bouville A, et al. The Chernobyl disaster: cancer following the accident at the Chernobyl nuclear power plant [J]. *Epidemiologic Reviews*, 2005, 27: 56-66.

[4] Nagatani K, Kiribayashi S, Okada Y, et al. Emergency response to the nuclear accident at the Fukushima Daiichi nuclear power plants using mobile rescue robots [J]. *Journal of Field Robotics*, 2013, 30(1): 44-63.

[5] Feng C, Wang C Z, Zhao J P, et al. Research status and key technologies analysis of operating robots for nuclear environment [J]. *Opto-Electronic Engineering*, 2020, 47(10): 88-98. (in Chinese)

[6] Christie G A, Shoemaker A, Kochersberger K B, et al. Radiation search operations using scene understanding with autonomous UAV and UGV [J]. *Journal of Field Robotics*, 2017, 34(8): 1450-1468.
[7] Li Z G, Chen W H, Liu C J. Review of UAV-based autonomous search algorithms for hazardous sources [J]. *Scientia Sinica (Informationis)*, 2022, 52(9): 1579-1597.
[8] Xu T L, Chen G D, Zhou G Q, et al. Fast source seeking with obstacle avoidance via extremum seeking control [C]//2022 13th Asian Control Conference (ASCC). Piscataway, NJ: IEEE, 2022: 2097-2102.
[9] Ramírez-llanos E, Martínez S. Stochastic source seeking for mobile robots in obstacle environments via the SPSA method [J]. *IEEE Transactions on Automatic Control*, 2019, 64(4): 1732-1739.
[10] Chen G D, Yuan S, Zhu X Z, et al. Path planning for fast swarm source seeking in unknown environments [J]. *International Journal of Adaptive Control and Signal Processing*, 2024, 38(2): 360-377.
[11] West A, Tsitsimpelis I, Licata M, et al. Use of Gaussian process regression for radiation mapping of a nuclear reactor with a mobile robot [J]. *Scientific Reports*, 2021, 11(1): 13975.
[12] Zhang C, Xiao Y F, Liu H J, et al. Search method of radioactive source based on particle filter and artificial potential field [J]. *Nuclear Physics Review*, 2020, 37(4): 867-874.
[13] Hutchinson M, Liu C J, Thomas P, et al. Unmanned aerial vehicle-based hazardous materials response: information-theoretic hazardous source search and reconstruction [J]. *IEEE Robotics &Automation Magazine*, 2020, 27(3): 108-119.
[14] Zhu H B. Research on source search and localization with mobile robots in unknown environments [D]. Harbin: Harbin Institute of Technology, 2022. (in Chinese)
[15] Long Z Y, Liu Y K, Yang L Q, et al. Study on localization method of radioactive source based on point kernel integration [J]. *Applied Science and Technology*, 2020, 47(6): 78-83.
[16] Tan Y, Yang J, Chen W H, et al. Multistep dual control for exploration and exploitation in autonomous search with convergence guarantee [J]. *IEEE Transactions on Industrial Informatics*, 2024, 20(6): 8207-8217.
[17] Li Z G, Chen W H, Yang J. Concurrent active learning in autonomous airborne source search: dual control for exploration and exploitation [J]. *IEEE Transactions on Automatic Control*, 2023, 68(5): 3123-3130.
[18] Prokhoretsi M, Prokhorets S I, Khazhmuradov M A, et al. Point kernel method for radiation fields simulation [J]. *Nuclear Physics Investigations*, 2007, 78(48): 106-109.

基于改进 SPSA 的组合驱动放射源搜寻算法

李冠汝[1], 胡 俊[2,3*], 虞 宙[2], 朱世杰[4]
1. 东华大学 机械工程学院, 上海 201620
2. 东华大学 人工智能研究院, 上海 201620
3. 东华大学 人工智能研究院, 纺织工业人工智能技术教育部工程研究中心, 上海 201620
4. 东华大学 信息与智能科学学院, 上海 201620

摘 要: 针对现有屏蔽物环境下放射源搜寻算法匮乏的问题, 本文提出了一种基于改进型同步扰动随机逼近(simultaneous perturbation stochastic approximation, SPSA)算法的组合驱动算法。该方法通过改进单边正交扰动向量, 并引入动态步长调整策略, 有效提升了算法的收敛性能; 为了解决复杂环境下规划路径失效的问题, 设计基于广度优先搜索的目标点修正机制, 实现了障碍物环境下目标点的动态校正与可行性保证。针对屏蔽物存在下的多空间场景, 提出探索状态切换机制, 可主动探索未观测区域。为了评估所提算法在收敛性能、障碍物适应性和探索能力方面的性能, 在 Gazebo 中建立了三个仿真环境, 分别代表以下环境: 开阔场地环境、复杂环境和辐射屏蔽环境。实验结果表明, 该算法在收敛性能方面优于标准 SPSA 算法和粒子滤波算法, 同时在复杂环境中也表现出良好的搜索能力。此外, 当面临屏蔽环境时, 本文所提算法展现出受阻后快速恢复对未知环境的主动探索能力。

关键词: 源搜寻算法; 同步扰动随机逼近; 组合驱动算法; 主动探索